SPACECRAFT CHARGING DURING ELECTRON BEAM INJECTION AND TURN-OFF

R. M. Winglee

Department of Astrophysical, Planetary and Atmospheric Sciences

University of Colorado, Boulder, CO 80309-0391

Abstract. During electron beam injection, particularly at currents exceeding about 100 mA, the spacecraft can become positively charged with potentials as high as the beam energy being observed. After beam turnoff, the spacecraft can become negatively charged. Two-dimensional electromagnetic particle simulations are used to investigate the characteristics of the spacecraft charging, particle acceleration and wave emissions during beam injection and turnoff. It is shown that during beam injection, the beam current is neutralized by a spatially separate return-current region extending several tens of meters from the beam region, with the currents being closed across the field lines by the perpendicular acceleration of ambient plasma ions into the beam region. At beam turn-off, this current system reverses, leading to (i) extended electron collection by the spacecraft near the beam region, (ii) preferential ion collection by sections of the spacecraft magnetically connected to the initial return current regions and (iii) the creation of hot plasma extending well into the return current regions. Collisional effects are shown to reduced the magnitude of the potential swing, as well as the extent of the heating of the ambient plasma.

1. Introduction

During electron beam injection, the spacecraft can become charged up to about the beam energy, particularly for currents exceeding about 100 mA and low plasma densities. Examples of experiments where such strong charging is observed include the SEPAC experiment on the Spacelab 1 [*Obayashi et al.*, 1985; *Sasaki et al.*, 1986] and the recent sounding rocket experiments CHARGE 2 and ECHO 7 experiments [*Banks et al.*, 1988; *Winckler et al.*, 1989]. This spacecraft charging is important as it can modify the properties of the beam as it tries to propagate away from the spacecraft, thereby modifying the beam-plasma interaction. The level of spacecraft charging is also dependent on the presence of neutrals in the near vicinity of the spacecraft. Observations showing large reductions in spacecraft potential during neutral thruster firings have been reported by *Banks et al.* [1988], *Gurnett et al.* [1988], *Gilchrist et al.* [1989] and *Winckler et al.* [1989].

Several particle simulations have been performed in an effort to understand some of the above observations and the properties of the beam-plasma interaction [e.g., *Winglee and Pritchett*, 1987, 1988; *Pritchett and Winglee*, 1988]. These initial simulations were electrostatic and collisionless with emphasis on determining the conditions under which the beam can escape with minimum distortion and the properties of the return currents and electrostatic wave emissions. More recently, electromagnetic [*Winglee and Kellogg*, 1989] and collisional [*Winglee*, 1989; *Chin et al.*, 1989] effects have been included to allow more complete modelling of the induced wave emissions and the modelling of the injection of neutrals via thruster firings. These simulations were able to account for some of the observed properties of the beam and wave emissions during ECHO 7.

The above observations and simulations have concentrated primarily on beam injection. To date, processes induced as the beam is turned off have received little attention. Such processes are nevertheless important as they can modify the

spacecraft charging and the local plasma environment which can in turn affect the beam-plasma interaction and spacecraft charging during subsequent beam injections. Such effects are of particular importance during pulsed beam injection. The purpose of this paper is to investigate the properties of the beam and spacecraft charging during electron beam injection and turn-off in both collisionless and collisional plasmas, using two-dimensional (three velocity) electromagnetic particle simulations.

In section 2, the simulation model is described. In section 3, the particle dynamics for injection into an essentially collisionless plasma is discussed. Differences in the particle dynamics due to the presence high neutral densities are discussed in section 4. The spacecraft potential and induced wave fields for injection into collisionless and collisional plasmas are presented in section 5. A summary of results is given in section 6.

2. Simulation Model

In order to investigate the beam-plasma interaction and spacecraft charging during beam injection and turn-off, the Beams-In-Geospace including Electromagnetic Radiation code (BIGER) which is two-dimensional (three velocity) relativistic electromagnetic particle simulations with collisional processes included was utilized [cf., *Winglee*, 1989]. A schematic of the simulation model is shown in Figure 1. The spacecraft is indicated by the rectangle and immersed in a plasma of uniform density which is typically 10^4 - 10^5 cm^{-3} for most active beam experiments. The spacecraft size is taken to be $4\Delta \times 32\Delta$, with the system size being $512\Delta \times 128\Delta$, where Δ is two plasma Debye length (i.e., $2v_{Te}/\omega_{pe}$). For the parameters considered here $\Delta \simeq$ 10–20 cm. The beam is injected at 45 degrees to the ambient magnetic field (which is in the x direction) with a parallel velocity 10 times the ambient electron thermal velocity (i.e., $v_{xb} = 10v_{Te} = 0.17c$) and a beam width of 2Δ. This beam

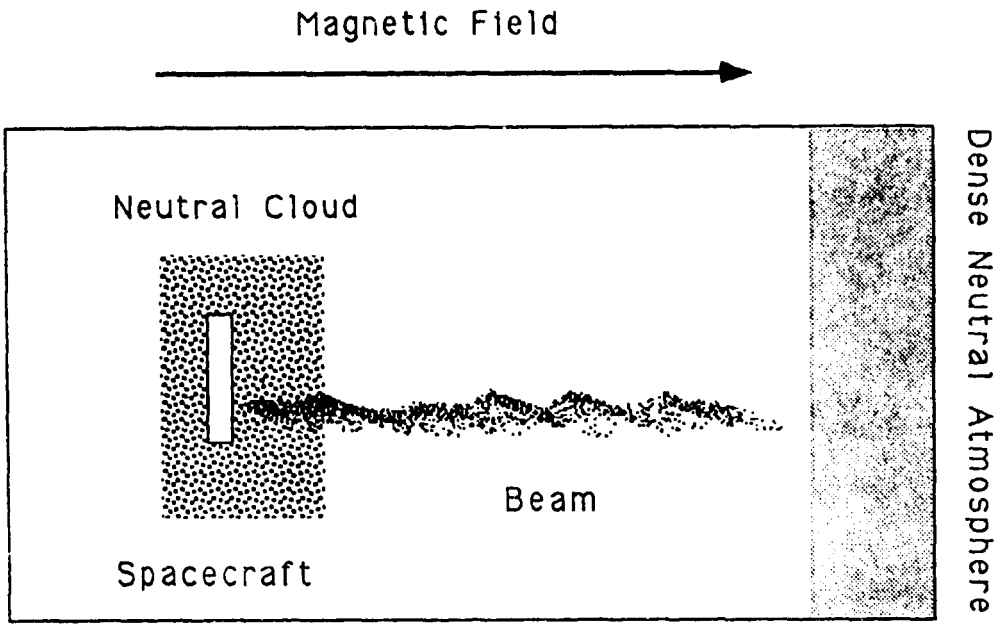

Figure 1. Schematic diagram of the simulation model.

width is the minimum beam width that can be easily simulated and represents some initial expansion of the beam within the first few tens of centimeters, due to the opening or cone angle of the gun and/or to beam-plasma interactions. As a result of the large beam width assumed in the simulations, the beam density relative to the ambient density assumed to be 4 with the total beam current being similar to the maximum beam current emitted during CHARGE 2, i.e. about 100 mA. The ratio of the electron cyclotron frequency Ω_e is assumed to be equal to ω_{pe}, similar to the plasma conditions during CHARGE 2. These parameters are also similar to those used in previous simulations by *Winglee and Pritchett* [1988] and *Winglee* [1989] except that the relative spacecraft size is twice as large, which reduces the amount of spacecraft charging and allows more of the beam to propagate outwards.

The effects of neutrals and their ionization are incorporated into the simulations as follows. A region of neutrals with a given density is specified on the simulation grid. These neutrals (assumed to be molecular nitrogen) can be placed

around the mother or daughter. A dense neutral region is also placed near the right hand boundary representing the lower ionosphere. The electrons and ions are subjected to elastic scattering collisions with cross-sections as given by *Strickland et al.* [1976]. In addition to these collisions, energetic electrons ($\gtrsim$ 100 eV) are subject to ionizing (inelastic) collisions. The ionization cross-section as given by *Banks and Kockarts* [1973] has the feature that it increases rapidly once the electron energy is above a few tens of eV, reaching a maximum at about 100 eV and then decreasing approximately inversely proportional to v. For numerical simplicity, the rise in ionization cross-section at low energies is approximated by a sharp cutoff at 100 eV (i.e., $v \simeq 3.3 v_{Te}$). This cutoff excludes ionization processes by nonaccelerated ambient plasma electrons which are assumed to be in equilibrium with the ambient neutrals. This cutoff has the effect of underestimating the number of low energy electrons produced by ionizing collisions. This approximation is not restrictive since these low energy electrons have a large scattering cross-section which reduces their mobility and hence their contributions to any return currents.

All electrons with higher energies above 100 eV are then binned in levels of speeds relative to $3.3 v_{Te}$, with the cross-section decreasing inversely with bin number. The required number of (primary) electrons determined from the collision cross-section is then chosen randomly from each bin. The velocity of the primary is reduced by about a third and a secondary electron and ion are added to the system with the secondary electron having a velocity one third of the initial velocity of the primary with a differential scattering cross-section as given by *Mott and Massey* [1965].

In the following there is always a neutral cloud placed around the spacecraft. In the first case, the collision period is long compared with the duration of the beam injection ($\nu = 1.25 \times 10^{-3} \omega_{pb}$ where ω_{pb} is the beam plasma frequency which corresponds to a neutral density $n_n \simeq 6 \times 10^{10}$ cm^{-3}) and is hereafter referred to as

"collisionless". In the second case, hereafter referred to as "collisional" the collision period is compared to the beam injection period, i.e $\nu = 2 \times 10^{-2} \omega_{pb}$, $n_n \simeq 1 \times 10^{12}$ cm^{-3}. In both cases, beam injection at constant current occurs during the period $0 \leq \omega_{pb} t \leq 120$.

3. Particle Dynamics For Beam Injection into a Collisionless Plasma

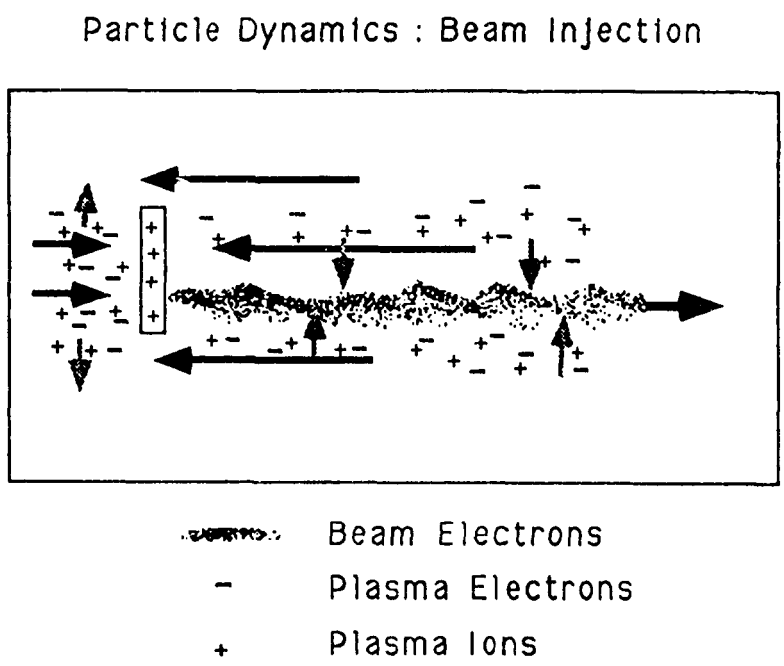

Figure 2. Schematic of the beam-plasma interaction during beam injection.

The dynamics of the beam-plasma interaction when the beam is on is shown schematically in Figure 2. The figure is derived from previous simulations results of *Pritchett and Winglee* [1987] and *Winglee and Pritchett* [1988]. During beam injection, the spacecraft becomes positively charged and return currents flow along the regions adjacent to the beam region, as well as from behind the spacecraft. Because the beam and return currents are spatially separate, plasma ions are accelerated across the field lines into the beam region to produce current closure. As shown in the following, after beam turn-off, the spacecraft can become negatively charged

due to an overshoot of return current into the spacecraft and the beam region can become positively charged due to the outflow of beam electrons. As a result, the electric fields and associated current system reverses, leading to strong deceleration of beam particles in the trailing edge of the pulse, and the formation of high energy tails in the ambient plasma in the return-current regions.

The evolution of the beam phase space is shown in Figure 3. At the earliest of times (Figure 3a), the ambient plasma is unable to respond to the beam injection and a virtual cathode or stagnation region develops, with many of the beam particles being reflected (i.e., attaining negative velocities) toward the spacecraft. At later times when the ambient plasma is able to respond to the injection and reduce the spacecraft charging (Figures 3b and c), a larger fraction of the beam is able to propagate outwards, although it is strongly distorted, as evidenced by large velocity spread at $x/\Delta \gtrsim 150$ and the vortex structure (or space-charge oscillation) at $x/\Delta \simeq 140$.

At beam turn-off, the outflowing beam electrons are no longer replaced by freshly injected electrons, so that a space-charge field is induced between these electrons and the ions left behind in the beam region. This space-charge field inhibits further outflow of beam electrons and in fact prevents some of the beam electrons emitted in the trailing half of the pulse from escaping from the near environment of the spacecraft (Figures 3d-f). Moreover, many of the beam electrons continue to overshoot into the spacecraft which causes, in part, the negative charging of the spacecraft.

At later times (Figures 3e and f), the energy of the inflowing beams electrons is seen to decrease. Note their maximum speed is rippled in space due to their interaction with induced wave turbulence and this rippling is convected back to the spacecraft. As a result, the energy of the electrons approaching the spacecraft varies in time, so that during periods where low energy electrons are arriving at

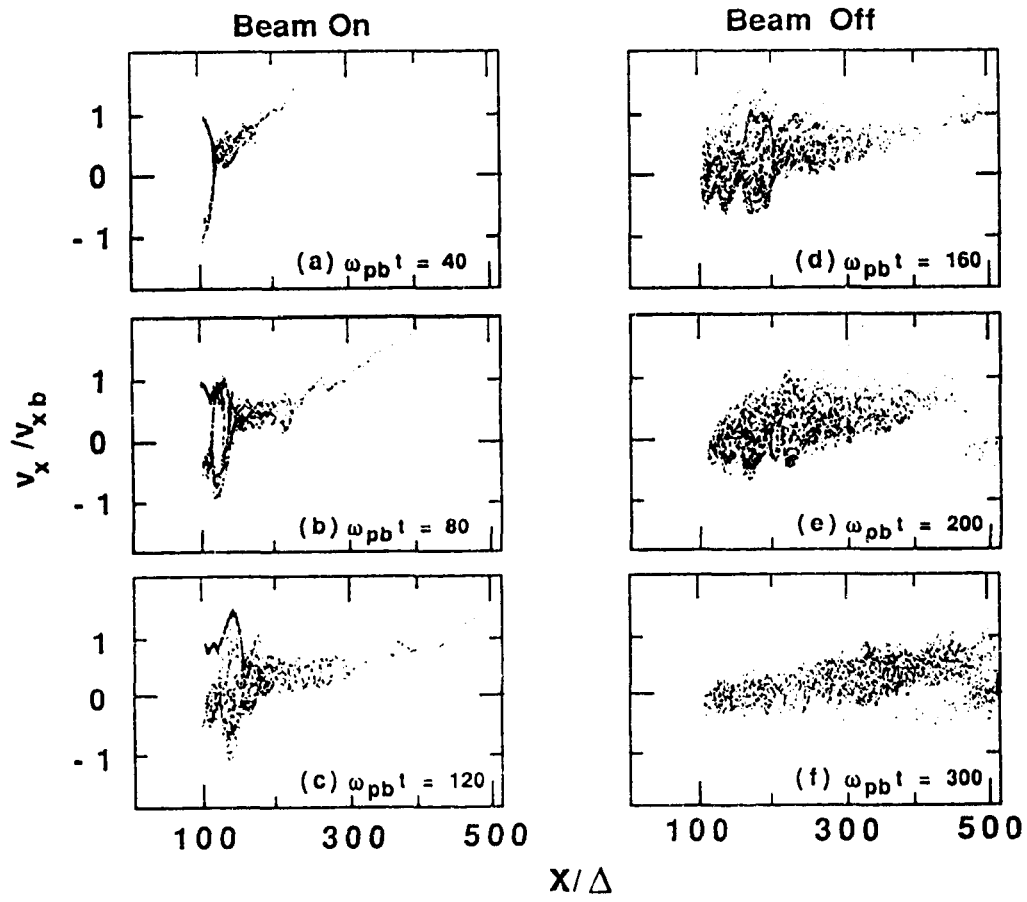

Figure 3. The $v_x - x$ phase space of the beam electrons

the spacecraft, its potential is able to reflect the electrons and slow its collection of negative charge. However, when the higher energy electrons arrive at the spacecraft that they are not reflected and the negative charge on the spacecraft charging can increase. Thus, the effect of the wave turbulence and its convection toward the spacecraft, causes the spacecraft potential to fluctuate and to remain at a net negative value over a much longer period than it would to a simple negative charged body to discharge (see section 5).

The properties of the plasma electrons, including the return-current electrons, is illustrated in Figure 4 which shows their field-aligned velocity v_x for a cut across the field lines between 60 and 180 Δ in front of the spacecraft. The

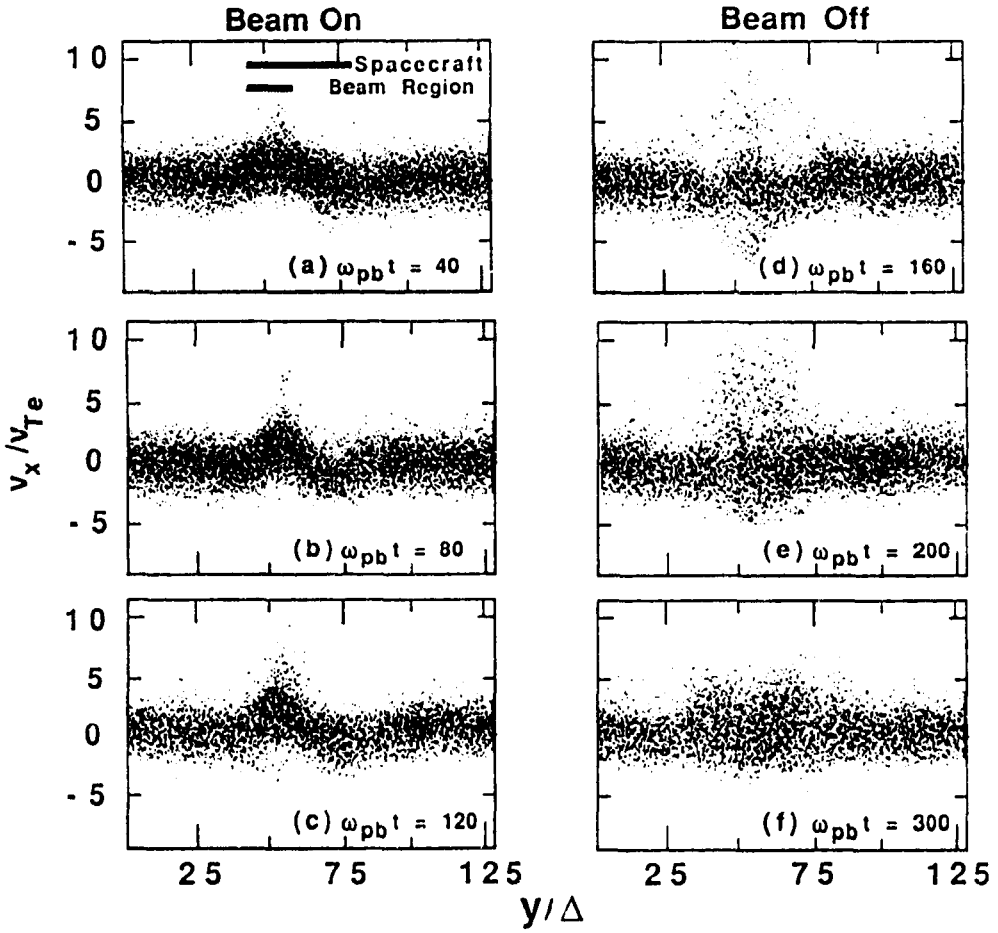

Figure 4. The $v_x - y$ phase space of the plasma electrons showing a cut across the field lines from 60 – 180 Δ in front of the spacecraft. Positive velocities indicate flow away from the spacecraft and negative velocities represent flows toward the spacecraft. The positions of the beam region and spacecraft are indicated in (a).

positions of the beam and spacecraft are indicated by the dotted and solid lines, respectively. During beam injection, electrons in the beam region are accelerated outwards reaching maximum velocities approximately equal to the beam parallel velocity. On adjacent field lines, electrons are accelerated toward the spacecraft (negative velocities), with those electrons magnetically connected to the spacecraft having the highest negative velocities of about -4 $v_{Te} = -0.4v_{xb}$ (Figure 4c).

At beam turnoff, these return current electrons continue to flow into the spacecraft (Figure 4d) until it is sufficiently negatively charged so that it reflects these electrons and eventually they attain positive velocities (Figures 4e and f). In addition, with the reversal of the current, those electrons in the return current regions with positive velocities at beam turn-off are seen to be accelerated to moderately high velocities ($v \gtrsim 5v_{Te}$), producing a hot electron region well outside the initial beam region.

Within the beam region, the velocity of many of the electrons is seen to reverse after beam turn-off, similar to the beam electrons. The speed of these electrons tends to be much greater than those of the return-current electrons, primarily due to (i) the large potential needed to stop the outflow of the beam electrons and (ii) the large amplitude turbulence excited by the beam electrons. Due to their relatively high velocity, there is a net flow into the spacecraft well, after the flow in the return-current regions have ceased (Figure 4f).

The ion motion across the field lines is illustrated in Figure 5 which shows the ion perpendicular velocity v_y for the same region as in Figure 4. The motion into the beam region during injection is seen as increase in v_y for ions below the beam region (i.e., small y) and negative increase for those ions above the beam region (i.e., large y; Figures 5a–c). The energy attained by these ions is comparable to the return-current electrons.

At beam turnoff, the beam region develops a positive charge excess due to the outflow of beam electrons, as discussed above. This change in sign causes the electric field driving the cross-field ion motion to reverse. As a consequence, the ions that were beginning to enter the beam region are reflected whereas, the ions which are near the beam center at turn-off are accelerated outwards (Figures 5e and f). This latter effect causes further acceleration of some of the ions up to energies comparable to the beam energy. These energetic ions continue outward

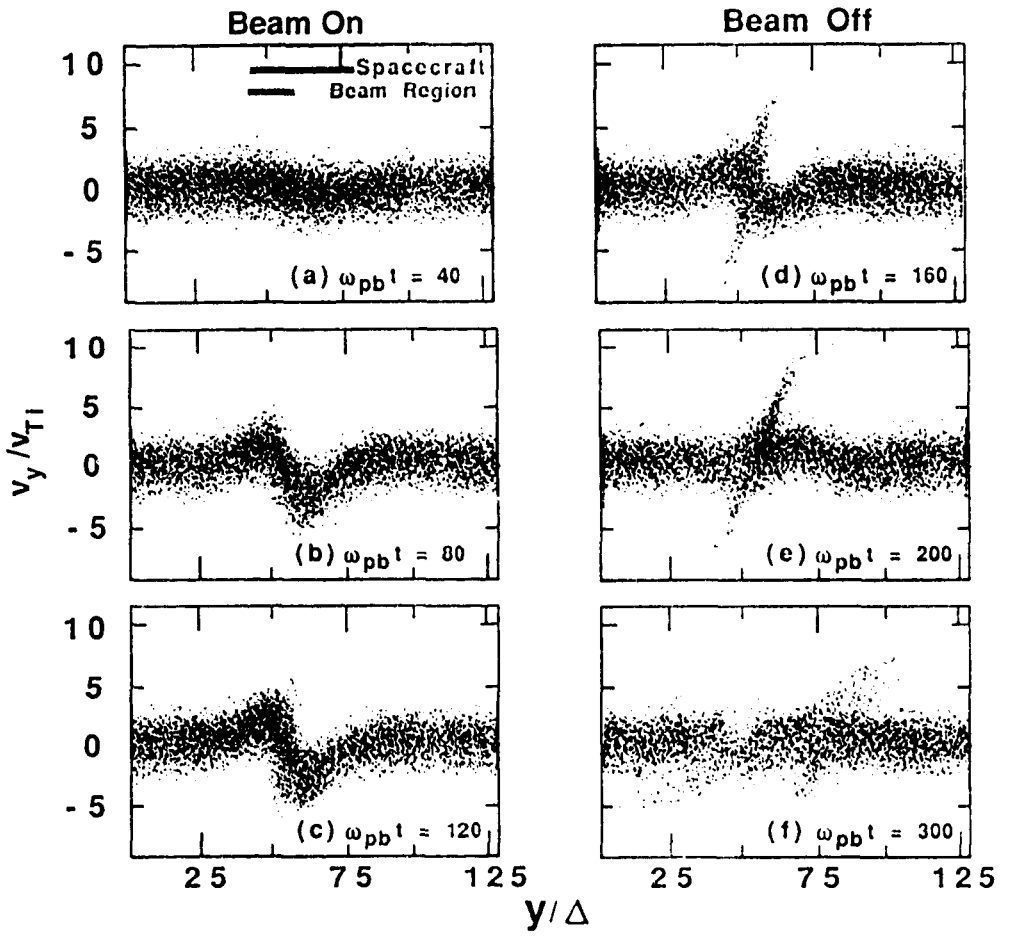

Figure 5. The $v_y - y$ phase space of the plasma ions for the same region as Figure 4.

into the return current regions, creating a hot population of ions well outside the beam region. The presence of such an extended region of hot plasma is consistent with observations from the Echo series [*Arnoldy et al.*, 1985; *Winckler et al.*, 1986, 1989].

The above properties of the induced plasma flows at beam turn-off are shown schematically in Figure 6. These flows are essentially a reversal of those during beam injection. However, as shown above, some plasma which is moving in the same

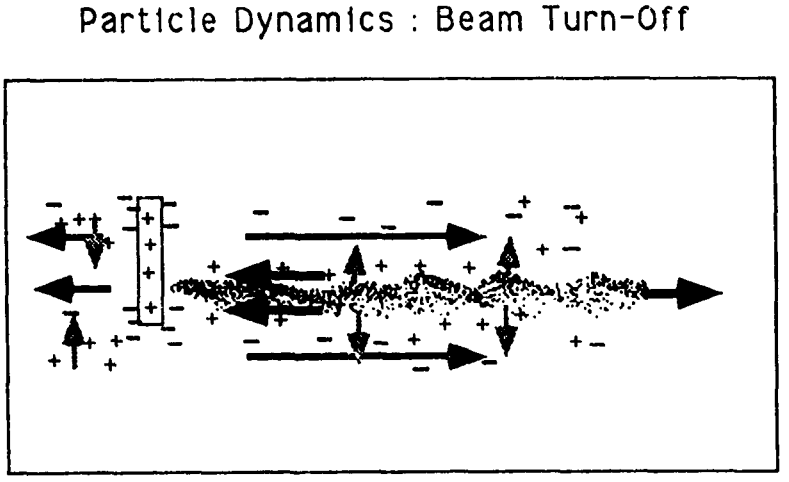

Figure 6. Schematic of the beam-plasma interaction during beam turn-off.

direction as the field reversal can attain high energies leading to the appearance of hot plasma regions well outside the beam region.

4. Collisional Effects

Figure 7 illustrates the change in the characteristics of the electron dynamics in the presence of high neutral densities which shows the beam and plasma electron phase spaces starting at the end of beam injection. Due to the choice of a relatively low charging-beam configuration and short period of beam injection, there is little difference in the phase spaces during injection (Figures 7a and d), except that there is enhanced electron densities in the beam region due to beam ionization of neutrals which results in (i) a reduction in the maximum energy attained by the plasma electrons, (ii) a return current which is more closely confined to the beam region and (iii) and an enhancement of short-scale turbulence in the beam region.

At beam turn-off, the development of high speed electrons in the beam and return current regions is suppressed. This is due to scattering collisions between the low energy particles and the neutrals. In the collisionless case, the unconstrained inflow of these particles causes the negative charging of the spacecraft. In the present

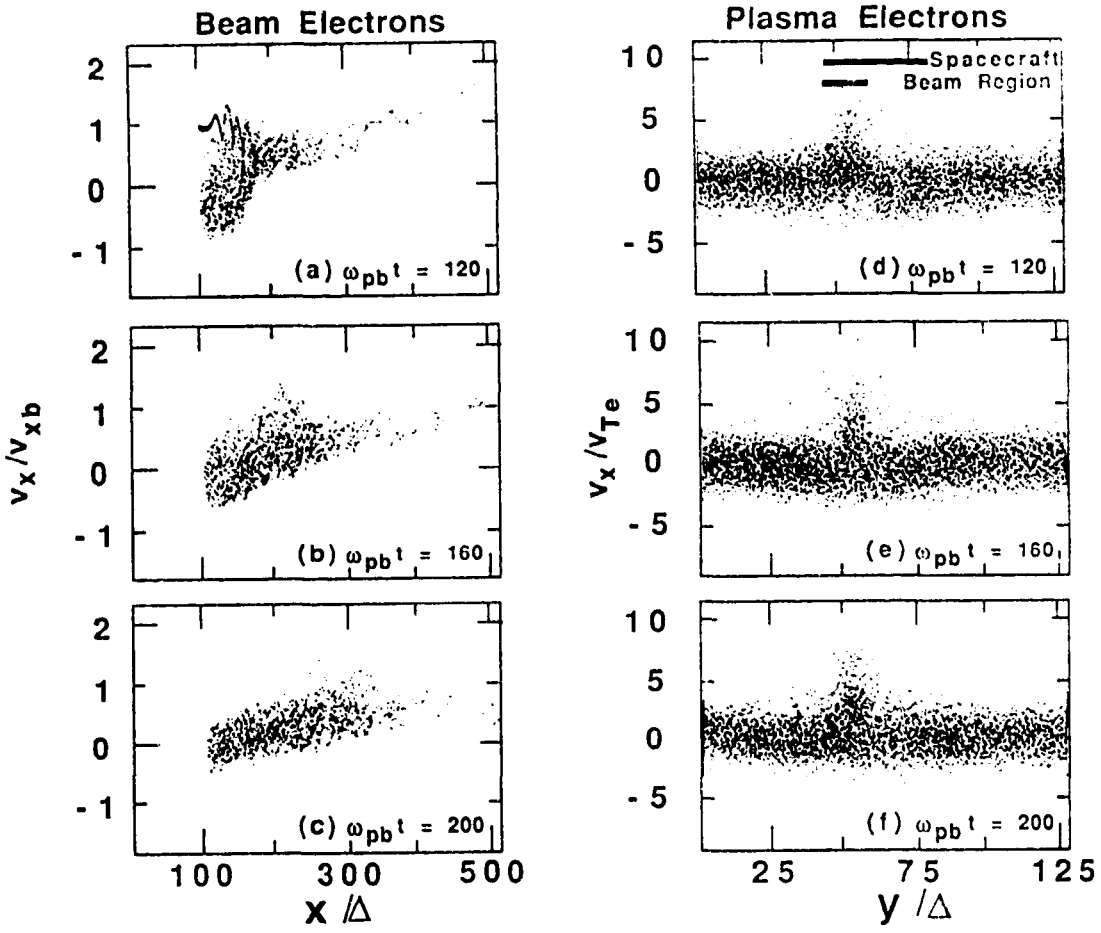

Figure 7. Electron phase spaces for the collisional case for the same regions as in Figures 3 and 4. At beam turnoff, the swing in electric field is reduced leading to a reduction in the heating of the plasma particle.

case, their flow is impeded by collisions and the large overshoot in current collection does not occur. As a result, the swing in electric field is not as large, thereby reducing the heating of the plasma at beam turn-off. This reduction in heating is seen in Figure 7e and f where the return current regions have a very much smaller temperature than in Figure 4. Note also that the region of hot ambient electrons

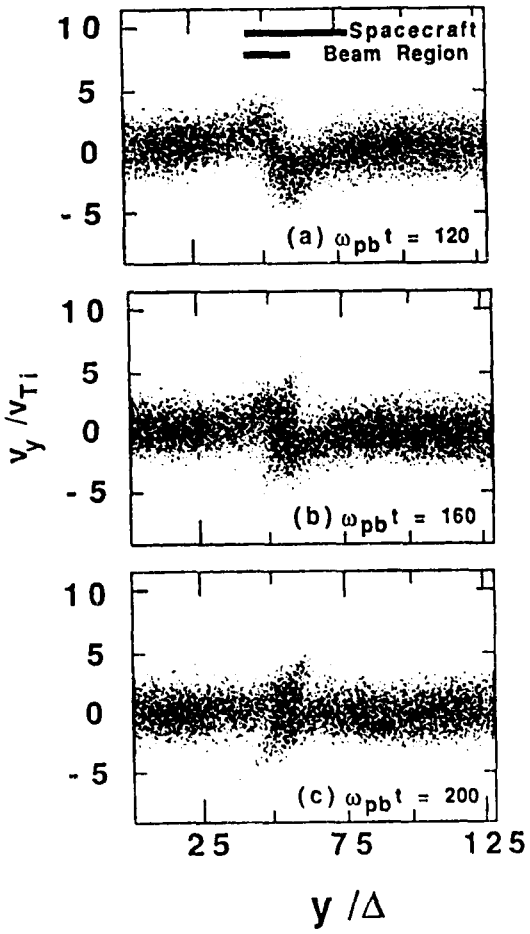

Figure 8. The ion $v_y - y$ phase space corresponding to the example in Figure 7.

is much more closely confined to the beam region compared with the collisionless case.

The reduction in the swing in the electric field at beam turn-off also suppress the acceleration of the ambient ions. This reduction is illustrated in Figure 8 which shows the ion $v_y - y$ phase space for the same times and region as in Figure 7. It is seen that the overall evolution is similar, with the ions moving into the beam region during injection and out of the region after turnoff. However, the maximum velocity attained by the ions is about half as small. With the reduction in the ion acceleration, the ions are unable to propagate as far across the field lines (which

is proportional to their gyroradius and hence velocity) so that the heated region of plasma ions and electrons appears closer in to the beam region, as it is for the electrons.

5. Spacecraft Potential and Wave Emissions

Time histories of the spacecraft potential for the collisionless and collisional cases are shown in Figure 9. The potential shortly after beam injection starts ($\omega_{pb}t \lesssim 20$) is approximately the same for the two cases, since there is insufficient time for the ambient plasma to respond to the injection nor to produce substantial ionization of the neutrals. At later times ($20 \lesssim \omega_{pb}t \lesssim 120$), the potential in the collisionless case tends to increase on average, although it is modulated by large amplitude oscillations associated with the space-charge fields induced by the beam injection.

At beam turn-off, there is an overshoot of electrons into the spacecraft as discussed above. This overshoot drives the spacecraft potential negative reaching a peak amplitude of 75% of the parallel beam energy which is nearly twice the magnitude of the potential during beam injection. This high potential is due to the inflow of energetic beam electrons. The potential remains approximately constant until $\omega_{pb}t \simeq 200$. After this time, ion collection by the spacecraft is able to reduce the negative charging with the magnitude of the potential reaching a local minimum at $\omega_{pb}t \simeq 240$. However, with the reduction in potential, hot electrons are again able to flow into the spacecraft (section 3) so that there is an increase in the magnitude of potential at $\omega_{pb}t \gtrsim 250$ and the spacecraft is unable to reach zero potential by the end of the simulation.

In the collisional case, the potential is also modulated but to a lesser extent due to collisional damping via the neutrals. Moreover, during beam injection the overall potential is reduced. The magnitude of the reduction would be larger if the

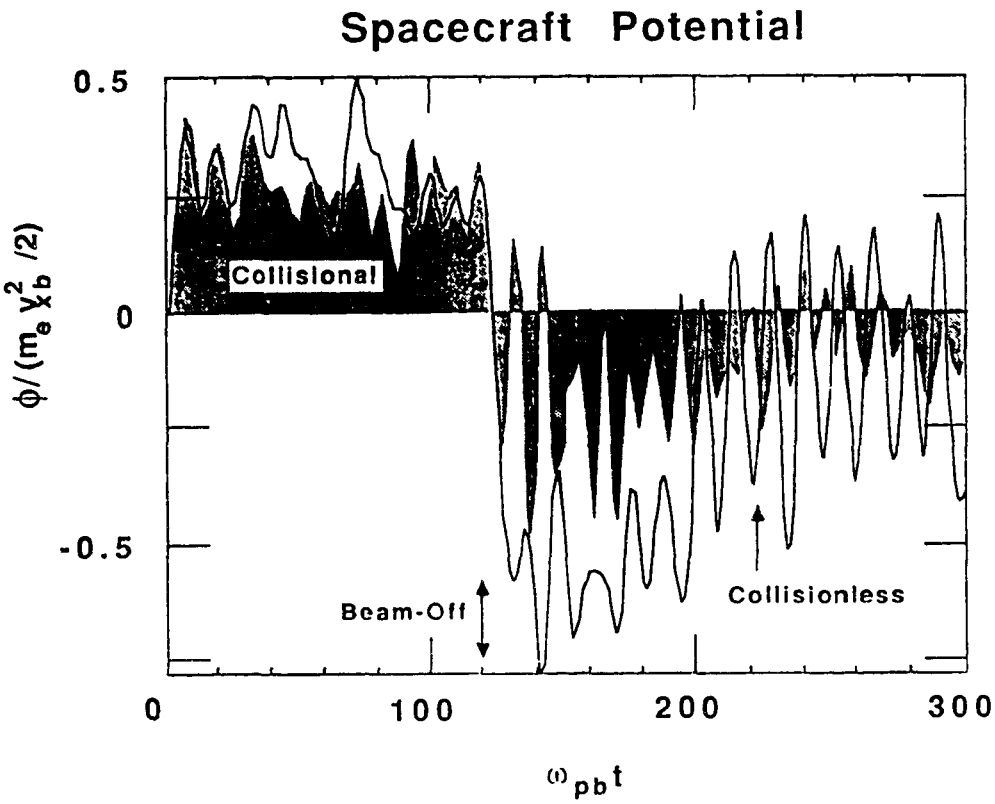

Figure 9. Spacecraft potential for the collisionless and collisional cases. The potential in the collisionless case is modulated by large amplitude oscillation during and after beam injection. These oscillations are reduced in the collisional case and the average potential is about half as small after beam turn-off.

beam injection was longer [cf. *Winglee*, 1989]. Here the beam is turned off at the point were the instantaneous potential for the two cases are approximately equal. At beam turn-off, the spacecraft becomes negatively changed as in the collisionless case, but the average spacecraft potential is about half as small. The collisional case is also similar in that the magnitude of the potential reaches a local minimum at $\omega_{pb}t \simeq 240$, after which the spacecraft becomes negatively charged due to further electron collection.

The time histories of the current collected by the spacecraft for the collisionless and collisional cases is shown in Figure 10. The current collected is divided into two parts, that which strikes the spacecraft on the lower half of the spacecraft from which the beam is emitted and the upper half of the spacecraft which is passive. In both cases, the beam emitting portion of the spacecraft collects most of the current at early times ($\omega_{pb}t \lesssim 60$). At later times during beam injection in the collisionless case, the passive section starts to collect a higher fraction of the current since electrons in the beam region are either collected on the spacecraft at early times or are accelerated forward (section 3). For beam injections of longer duration than shown, this collection can cause depletion of the ambient plasma, leading to a decrease in return current and an increase in spacecraft charging [cf. *Winglee*, 1989]. In the collisional case, the active section of the spacecraft collects a much larger percentage of the current due to a continual creation of electrons via ionization.

At beam turnoff, both proportions of the spacecraft collect net electron charge until about $\omega_{pb}t \simeq 140$ at which time the lower beam-emitting region is able to collect some net ion charge. This initial localization of the ion current is primarily due to the fact that the bulk of the ambient ions have been drawn into the beam region by the time the beam has been turned off. The upper passive region is only able to collect net positive charge after about $\omega_{pb}t \simeq 200$, which corresponds to the outflow of ions from the beam region (Figure 5).

At about the same time as the upper section starts to collect net ion current, the lower section starts to collect net negative electron current. This reversal in charge collected is not just coincidental but a necessary feature for closing the current system. Specifically, the ions in the beam region flow outward across the field lines while the electrons in the return-current regions flow away from the spacecraft. This electron flow is in part matched by an electron flow in the beam region toward the spacecraft. These electrons which are preferentially collected by the lower

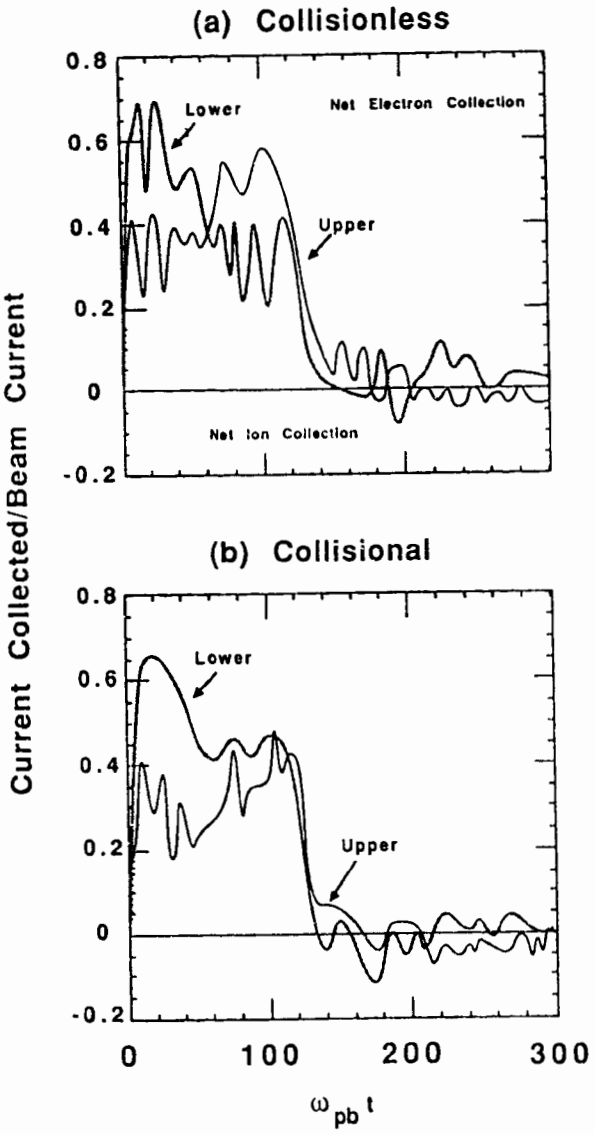

Figure 10. Time histories of the current collected by the spacecraft for the collisionless and collisional cases respectively. The dotted curves marked "lower" show the current collected by the beam-emitting lower portion of the spacecraft while the solid curve marked "upper" indicates that collected by the upper passive portion of the spacecraft where return current electrons most often strike the spacecraft.

section are then redistributed across the spacecraft (since it is an equipotential)

providing some cross-field current which partially offsets the plasma-ion current. In addition, ions must be collected by the spacecraft in order to reduce its charging. These ions must be collected by the passive section of the spacecraft with the skin of the spacecraft redistributing the charge to the lower active section in order to provide a balancing ion flow to match the plasma-ion current.

As indicated above, with beam turn-off there is a reversal of the fields and currents. This reversal is accompanied by a temporally increase in some of the electric field components in the system. This increase is illustrated in Figure 11 which shows the time histories of the dominant field components for the collisionless (left hand side) and collisional (right hand side) cases. The electrostatic fields are the most energetically important fields (Figures 11a and d). Shortly after beam turn-off, the energy in these fields in the collisionless case is seen to nearly double. This large increase is required in order to stop the outflow of beam particles. In the collisionless case, the parallel electrons field E_x increases by about the same amount but the increase in the perpendicular electric field E_y is substantially reduced. This reduction is due to the collisional damping of the overshoot in current collection by the spacecraft.

The magnetic field component B_z which is an indicator of the electromagnetic parallel currents in the system (middle panels) has a much slower rise time that the electrostatic fields. This slow rise time is in part due to the penetration of the current system into the plasma as well as due to the finite inductance of the plasma. At beam turn-off, the currents are reduced and the B_z fields decrease rapidly. The presence of collisions provide an extra mechanism for the dissipation of the electromagnetic currents so that the field energy in the collisional case in Figure 11e is smaller than that in Figure 11b. This is also true for the other electromagnetic field components (Figures 11c and f) which are drive by Hall currents (B_x) and by wave emissions, primarily whistlers.

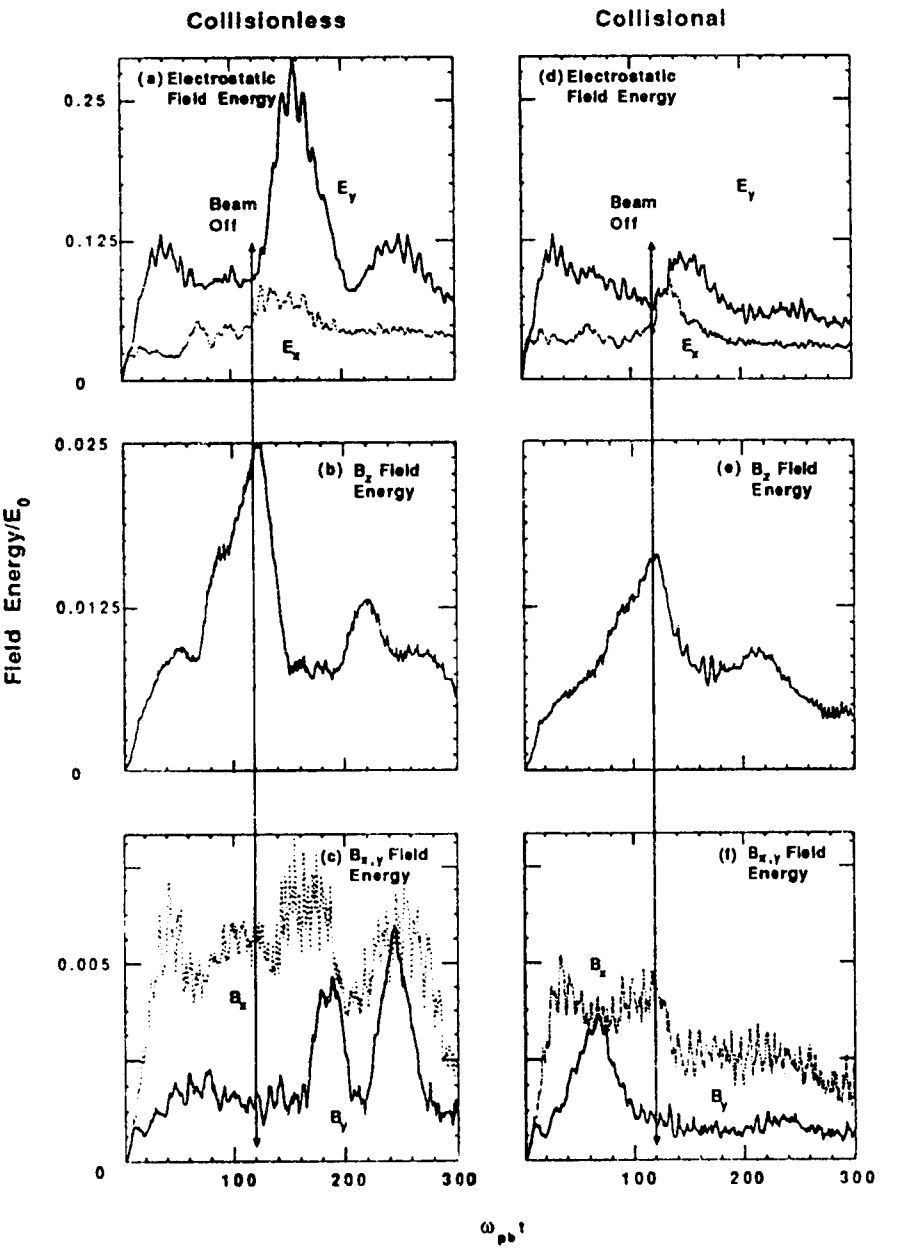

Figure 11. Time histories of the field energies for the collisionless and collisional cases. The electrostatic fields are energetically the most important. The energy of these fields tend to increase temporarily after beam turn-off, athough the increase in the perpendicular component is suppressed in the presence of high neutral densities.

As an example of the induced wave emissions across the system, Figure 12 shows the spectra of the perpendicular electric field taken 60Δ in front of the

spacecraft at points (a) centered in the beam region and (b) in the return current region 24Δ across the field lines from the beam region. Results for the collisionless case are shown on the left hand side and those for the collisional case on the right hand side. The spectra have been integrated over $200/\omega_{pb}$ on either side of beam turn-off.

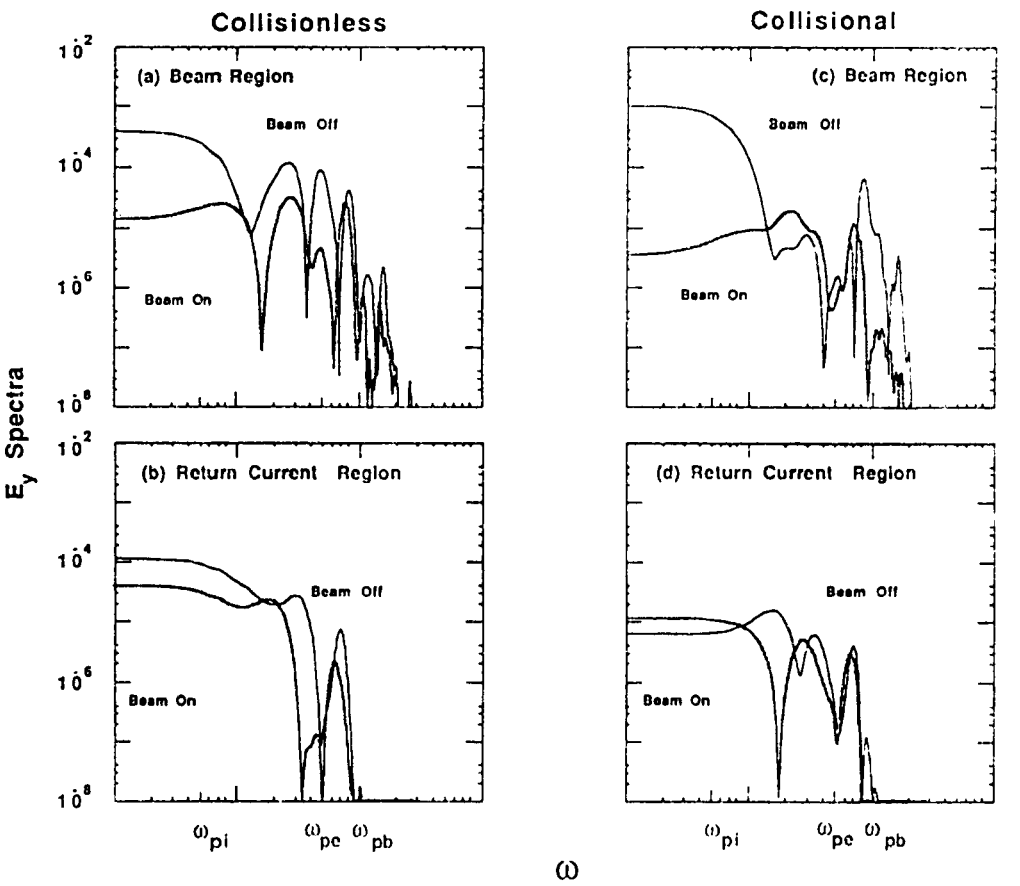

Figure 12. Wave spectra of the dominant field E_y in the beam and return-current regions during beam injection and turn-off. Results for the collisionless case are shown on the left hand side and those for the collisional case on the right hand side.

Broadband emissions are present in both the beam and return current regions, although the upper cutoff of the emissions is highest in the beam region and the waves are more intense. These waves include Langmuir, upper-hybrid and lower-hybrid waves. The spectra taken after beam turn-off for the collisionless case shows an increase over essentially the full range of frequencies in both the beam and return current regions. For the collisional case, there is primarily only an enhancement in the field strength in the beam region at the highest frequencies and in the quasi-static (low frequencies) fields, with little increase in the wave emissions in the return-current region. These differences are due to the collisional damping of the wave emissions and the closer confinement of the heated plasma to the beam region, as discussed above.

6. Summary

During electron beam injection, particularly at currents exceeding about 100 mA, the spacecraft can become positively charged with potentials as high as the beam energy being observed. After beam turnoff, the spacecraft can become negatively charged. Two-dimensional electromagnetic particle simulations are used to investigate the characteristics of the spacecraft charging, particle acceleration and wave emissions during beam injection and turnoff. It is shown that during beam injection, the beam current is neutralized by a spatially separate return current region extending several tens of meters from the beam region, with the currents being closed across the field lines by the perpendicular acceleration of ambient plasma ions in the beam region. Just after beam turnoff, the electrons in the return current regions continue to flow into the spacecraft due to their finite inertia causing the spacecraft to charge sufficiently negative to reflect these incoming electrons. Electrons in this region but travelling away from the spacecraft at beam turn-off are accelerated forward by the same electric field decelerating the incoming electrons

to energies of a few hundred eV, so that a hot plasma region appears well outside the beam region.

Within the beam region, a space-charge field develops between the outflowing beam electrons and the ions left behind. This electric field accelerates some of the ions drawn into the beam region outwards across the field lines to energies of the order of the beam energy. The same electric field causes many of the beam electrons injected near the end of the pulse to be decelerated and drawn into the spacecraft. These reflected beam electrons have sufficient energy to propagate through the spacecraft potential and reach the spacecraft so that there is negative-charge collection on the spacecraft near the beam region well after the beam is turned off. The negative charge of the spacecraft is eventually neutralized by ion flow into the spacecraft which preferentially occurs along the passive surfaces of the spacecraft magnetically connected to the original return current regions.

The presence of high neutral densities in the vicinity of the spacecraft can reduce the magnitude of the spacecraft charging during both beam injection and turn-off. This reduction is achieved by several interrelated processes. First, the ionization of the neutrals provides enhanced plasma densities for return currents into the spacecraft during beam injection and as a result the average energy of the return current electrons is reduced. Second, elastic scattering of the low-energy return-current electrons off the neutrals reduces the overshoot of electrons into the spacecraft at beam turn-off. Thirdly, there is suppression of quasi-static fields driving the currents as well as wave emissions, particularly outside the beam region. As a result of these processes, most of the heating of the ambient plasma is very much more closely confined to the beam region.

Acknowledgements.

This work was supported by NASA's Ionospheric Physics, Solar Terrestrial Theory and Solar Heliospheric Physics Programs under grants, NAGW-1587,

NAGW-91 and NSG-7287 and National Science Foundation grant ATM 87-19371 to the University of Colorado. The particle simulations were performed on the CRAY X-MP at the San Diego Supercomputer Center which is supported by the National Science Foundation.

References

Arnoldy, R. L., C. Pollock, and J. R. Winckler, The energization of electrons and ions by electron beams injected into the ionosphere, *J. Geophys. Res., 90*, 5197, 1985.

Banks, P. M., and G. Kockarts, *Aeronomy*, Academic Press, New York, Part A, 184, 1973

Banks, P. M., B. E. Gilchrist, T. Neubert, N. Myers, W. J. Raitt, P. R. Williamson, A. Fraser-Smith, and S. Sasaki, CHARGE-2 rocket observations of vehicle charging and charge neutralization, *Adv. Space Res.*, in press, 1989

Gilchrist, B. E., P. M. Banks, T. Neubert, P. R. Williamson, N. B. Myers, W. J. Raitt, and S. Sasaki, Observations of electron collection enhancement using neutral gas thruster jets on an isolated charged vehicle in the ionosphere, *Geophys. Res. Lett.*, in press, 1989.

Gurnett, D. A., W. S. Kurth, J. T. Steinberg, and S. D. Shawhan, Plasma wave turbulence around the shuttle: Results from the Spacelab-2 Flight, *Geophys. Res. Lett., 15*, 760, 1988.

Lin, C. S., J, Koga, and R. M. Winglee, Particle simulations of spacecraft charging by electron beam injection into a background of plasma and neutral gas, *Proc. Spacecraft Charging Technology Conference*, this volume, 1989.

Mott, N. F., and H. S. Massey, *The Theory of Atomic Collisions*, Oxford University Press, New York, 1965.

Obayashi, T., and 12 others, Initial results of SEPAC scientific achievement, *Earth Orient. Applic. Space Technol.*, *5*, 37, 1985.

Pritchett, P. L., and R. M. Winglee, The plasma environment during particle beam injection into space plasmas: 1. Electron beams, *J. Geophys. Res.*, *92*, 7073, 198.

Sasaki, S., N. Kawashima, K. Kuriki, M. Yanagisawa, and T. Obayashi, Vehicle charging observed in SEPAC Spacelab-1 experiment, *J. Spacecr. Rockets*, *23*, 129, 1986.

Strickland, D. J., D. L. Book, T. P. Coffey, and J. A. Fedder, Transport equation techniques for the deposition of auroral electrons, *J. Geophys. Res.*, *81*, 2755, 1976.

Winckler, J. R., Y. Abe, and K. N. Erickson, ELF waves and ion resonances produced by an electron beam emitting rocket in the ionosphere, in *Ion Acceleration in the Magnetosphere and Ionosphere*, Geophysical Monograph 38, AGU, 191, 1986.

Winckler, J. R., and 12 others, Echo 7: An electron beam experiment in the magnetosphere, *EOS, 70*, 657, 1989.

Winglee, R. M., and P. L. Pritchett, Space charge effects during the injection of dense electron beams into space plasmas, *J. Geophys. Res.*, *92*, 6114, 1987.

Winglee, R. M., and P. L. Pritchett, Comparative study of cross-field and field-aligned electron beams in active experiments, *J. Geophys. Res.*, *93*, 5823, 1988.

Winglee, R. M., and P. J. Kellogg, Electron beam injection during active experiments 1. Electromagnetic wave emissions, *J. Geophys. Res.*, in press, 1989.

Winglee, R. M., Electron beam injection during active experiments 2. Collisional Effects, *J. Geophys. Res.*, in press, 1989.